Contrib Mineral Petrol (1985) 91:340–353

Contributions to Mineralogy and Petrology

Polybaric differentiation of alkali basaltic magmas: evidence from green-core clinopyroxenes (Eifel, FRG)

Antje Duda* and Hans-Ulrich Schmincke
Institut für Mineralogie, Ruhr-Universität Bochum, D-4630 Bochum 1, FRG

Abstract. The Quaternary foidites and basanites of the West Eifel (Germany) contain optically and chemically heterogeneous clinopyroxenes, some of which occur as discrete zones within individual crystals: Most clinopyroxene phenocrysts are made up of a core and a normally zoned comagmatic titanaugite mantle. Most cores are greenish pleochroic and moderately resorbed (fassaitic augite). Some are pale green and strongly resorbed (acmitic augite). Cores of Al-augite composition and of Cr-diopside derived from peridotite xenoliths are rare. The fassaitic augites are similar in trace element distribution pattern to the titanaugites, but are more enriched in incompatible elements. The acmitic augites, in contrast, are clearly different in their trace element composition and are enriched in Na, Mn, Fe and depleted in Al, Ti, Sr, Zr. A model for polybaric magma evolution in the West Eifel is proposed: Primitive alkali basaltic magma rises through the upper mantle precipitating Al-augite en route. It stagnates and differentiates near the crust/mantle boundary crystallizing Fe-rich fassaitic augites. The magma differentiated at high pressure is subsequently mixed with new pulses of primitive magma from which the rims of pyroxene are crystallized. Sporadic alkali pyroxenite xenoliths are interpreted to represent cumulates of cognate phases formed within the crust and not metasomatized upper mantle material (Lloyd and Bailey 1975).

Introduction

Mafic alkalic basalts such as nephelinites, leucitites and basanites are commonly interpreted to represent relatively primitive partial melts from the upper mantle, having ascended relatively fast without significant modification en route. This interpretation is based on the primitive chemical composition of the rocks and the common occurrence of ultramafic xenoliths in the alkali basalts which are regarded as fragments of upper mantle peridotite.

Clinopyroxene is the dominant phenocryst phase in mafic alkali basalts from continental and oceanic intraplate tectonic settings. These clinopyroxenes are generally strongly zoned and many show optically distinct cores of variable chemical composition. Continuous and discontinuous, normal and inverse chemical zonation of clinopyroxenes in these rocks indicate a more complex magma evolution than is commonly envisaged, probably involving several magma batches and various intermediate evolutionary stages at different P, T, fo_2, etc.

Green Fe-rich cores within titanaugite phenocrysts are widespread in alkali basalts. They have been described from the Quaternary Eifel (e.g. Duda and Schmincke 1978; Mertes 1983; Duda 1984; Viereck 1984) and the Tertiary Eifel (Huckenholz 1965a, b, 1966, 1973), the Massif Central (e.g. Wass 1979a), Italian volcanic provinces (e.g. Civetta et al. 1979; Barton et al. 1982), ocean islands like Gran Canaria (e.g. Frisch and Schmincke 1969) and from K-rich rocks of Leucite Hills (Barton and Bergen 1981) and Uganda (Lloyd 1981). The common occurrence of these Fe-rich clinopyroxenes must indicate characteristic stages during the evolution of alkali basalts in general.

We have studied in detail the mineral chemistry of clinopyroxenes from most volcanic rock types throughout the entire Quaternary West Eifel volcanic field in order to assess the following problems:

(1) What are the characteristic stages of host magma differentiation that are reflected in the common occurrence of the Fe-rich clinopyroxenes cores?

(2) Is a single process sufficient to explain the different types of green clinopyroxene cores?

(3) What is the implication of the geological occurrence of these clinopyroxenes with respect to the evolution of mafic alkaline magmas in general?

The Eifel volcanic field (Fig. 1) is located on top of the Variscian Rhenish Shield which was uplifted since the Tertiary. This plateau was studied recently in detail by geophysical and geological methods (Fuchs et al. 1983). A petrogenetic model for the magmas of the West Eifel was proposed by Mertes and Schmincke (1985) based on field, petrographic and bulk rock chemical analyses. Radiogenic isotopes and REE geochemistry of these rocks will be presented elsewhere (Wörner et al., in prep.; Hertogen et al., in prep.). The West Eifel volcanic field comprises about 600 km^2 and 240 eruption centers. Volcanic activity started about 0.7 Ma before present (Mertes and Schmincke 1983) and the last eruption occurred about 10000 a ago (Büchel and Lorenz 1982).

Host rocks

Geochemistry

Primitive (MgO > 7 wt.%), SiO_2-undersaturated alkali-rich magmas are the most common lava type in the Quaternary West Eifel volcanic field. Two main magma suites are distinguished chemically

* Now: Abteilung Bauwesen, Universität Dortmund, D-4600 Dortmund 50

Offprint requests to: A. Duda

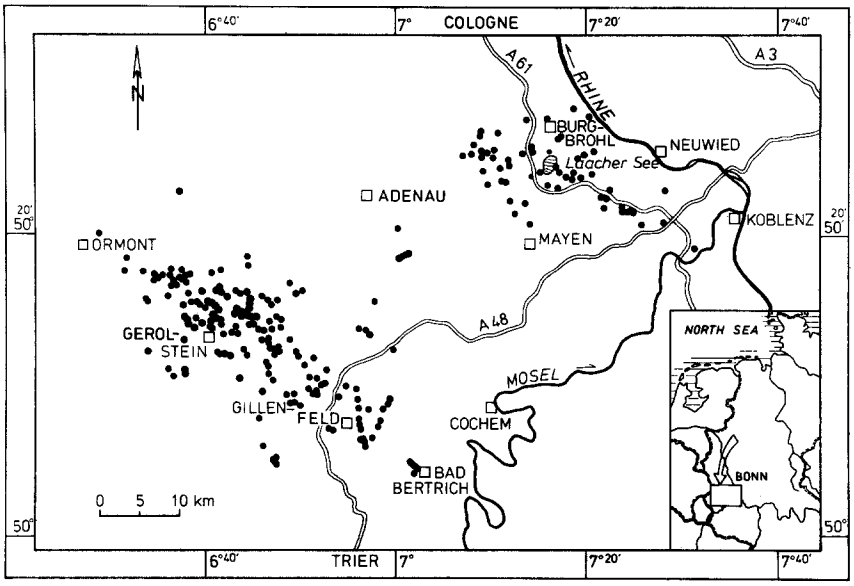

Fig. 1. Eruptive centers of the Quaternary East and West Eifel (Mertes and Schmincke, 1985)

Table 1. Average chemical composition of mafic (olivine-bearing) Quaternary West Eifel volcanics (Mertes and Schmincke 1985) in wt.% and ppm, resp.

No. of analyses	Mel-fr. Foidite 52	Mel-bear. Foidite 41	Olivine-Nephelinite 6	Basanite 9
SiO_2	42.6 ± 1.0	41.1 ± 0.8	41.8 ± 0.5	42.9 ± 0.5
TiO_2	2.8 ± 0.3	2.8 ± 0.2	2.7 ± 0.1	2.5 ± 0.1
Al_2O_3	12.2 ± 0.8	11.6 ± 0.6	12.3 ± 0.5	12.0 ± 0.2
Fe_2O_3	6.3 ± 1.6	7.2 ± 1.7	5.1 ± 0.9	3.9 ± 1.0
FeO	4.4 ± 1.4	4.3 ± 1.4	5.4 ± 1.4	7.2 ± 1.0
MnO	0.19± 0.02	0.21± 0.02	0.20± 0.01	0.19± 0.01
MgO	10.2 ± 1.0	10.4 ± 1.2	12.3 ± 1.1	13.1 ± 0.8
CaO	14.1 ± 0.7	15.0 ± 1.0	12.8 ± 0.3	12.1 ± 0.5
Na_2O	2.93± 0.51	3.25± 0.45	3.91± 0.60	3.14± 0.22
K_2O	3.33± 0.33	3.01± 0.41	2.28± 0.30	1.53± 0.09
P_2O_5	0.67± 0.11	0.89± 0.23	0.82± 0.09	0.92± 0.07
H_2O	0.72± 0.39	0.98+ 0.60	0.37± 0.42	0.35± 0.32
CO_2	0.12± 0.13	0.49± 0.63	0.06± 0.04	0.08+ 0.11
Cr	290 ±119	277 ±109	505 ± 84	535 ±72
Co	54 ± 13	54 ± 10	53 ± 6	67 ± 7
Ni	146 ± 42	136 ± 37	244 ± 66	296 ±31
Cu	130 ± 32	130 ± 33	68 ± 4	73 ± 5
Zn	79 ± 11	87 ± 12	89 ± 4	87 ± 3
Rb	102 ± 14	86 ± 16	63 ± 9	40 ± 4
Sr	887 ±166	928 ±276	1,157 ±100	989 ±98
Y	24 ± 2	28 ± 5	29 ± 1	28 ± 2
Zr	231 ± 26	262 ± 55	252 ± 22	205 ±14
Nb	86 ± 15	103 ± 23	111 ± 16	74 ± 8
Ba	1,180 ±105	1,202 ±130	1,201 ±227	872 ±58
Mg-No. × 100	67.0 ± 3.0	66.3 ± 3.1	71.3 ± 1.5	70.8 ± 1.5

and petrographically (Mertes and Schmincke 1985): (1) A dominant foidite suite (F-group) comprising nephelinites and leucitites and (2) an olivine-nephelinite and basanite suite (ONB-group) (Table 1). Small volumes of more differentiated (MgO < 7 wt.%) tephrites and phonolites occur only in the center of the field and were probably fractionated from the F-group magmas, judging from their spatial proximity and chemical affinity.

MgO-rich (MgO > 10 wt.%) magmas of both the F- and ONB-group are interpreted as nearly primary melts having experienced minor fractionation during ascent. They show parallel element variation trends, though the F-group magmas show higher concentrations of e.g. Rb, Ba, LREE and higher K_2O/Na_2O and CaO/Al_2O_3 ratios. These compositional differences and the spatial separation within the volcanic field indicate different mantle source domains for the two magma groups: a phlogopite-bearing garnet peridotite at about 100 km depth for the F-group magmas and an amphibole-bearing garnet-peridotite at about 60 km depth for the ONB-group magmas (Mertes and Schmincke 1985). Within one suite, different primitive magmas are interpreted to reflect different degrees of partial melting of the same source. Magmas with low Mg-values are interpreted to have fractionated clinopyroxene, olivine and minor phlogopite.

Table 2. Modal composition of the main Quaternary West Eifel volcanics (after Mertes 1983)

Magma group	Rock type	Phenocrysts			Major groundmass phases							
		Oliv.	Cpx	Phl, Amph	Oliv.	Cpx	Tm	Phl	Mel	Ne	Leuc.	Fsp
	Tephrite		+	(+)		++	+	+			++	++
F-group	Ol-free Foidite		++	(+)	(+)	++	+	+		++	++	
	Mel-free Neph., Leucitite	(+)	+		(+)	++	++	+		++	++	tr
	Mel-bear. Neph.	(+)	+		(+)	++	++	+	+	++	tr	
ONB-group	Ol-Neph.	+	(+)		+	++	+	tr		+		
	Basanite	+	(+)		+	++	+	tr		+		+

++ > 10 Vol.%; + > 5 Vol.%; (+) < 5 Vol.%; tr trace

Petrography of lavas

The modal composition of the main volcanic rock groups is given in Table 2. Clinopyroxene and olivine phenocrysts dominate the mafic rocks (MgO > 8 wt.%). Clinopyroxene (up to 25 Vol.%) exceeds olivine in the F-group while lavas of the ONB-group contain more olivine than clinopyroxene (> 2:1).

The clinopyroxene phenocrysts are subhedral to euhedral but are commonly heterogeneous: the core zone is typically greenish to brownish, resorbed and optically discontinuous compared to the pale colored zoned rim. The olivine phenocrysts, too, are subhedral to euhedral and contain inclusions of Cr-spinel (< 2 Vol.%) and titanomagnetite. In more evolved foidites, overgrowth of clinopyroxene and phlogopite around olivine is common. Phlogopite phenocrysts are less common.

Differentiated rocks such as tephrites also show heterogeneous clinopyroxene phenocrysts, although to a lesser extent, and also contain phenocrysts of amphibole, titanomagnetite and apatite. The matrix in these rocks mainly consists of clinopyroxene accompanied by titanomagnetite, feldspathoids and/or feldspar as well as olivine in the mafic and phlogopite in the more evolved F-group rocks.

Petrography of xenoliths

Ultramafic xenoliths less than 5 mm in size occur in about 70% of the ONB- and F-group (with MgO > 9 wt.%) volcanoes, i.e. 87% of the West Eifel eruptive centers. Larger ultramafic xenoliths up to 40 cm diameter are found in about 20% of the eruptive centers (Mertes 1983).

Two groups of ultramafics are distinguished. Lherzolite xenoliths are composed of Mg-rich olivine, orthopyroxene, Cr-diopside and minor Cr-spinel. Most xenoliths show evidence of melting along grain boundaries and glass and OH-bearing phases like Cr-bearing amphibole and/or phlogopite in pockets.

Alkali pyroxenites are characterized by the presence of Ti-augite, Cr-free amphibole and phlogopite and by the absence of orthopyroxene. Minor phases are titanomagnetite, apatite and sphene. The xenoliths exhibit clear cumulus but no deformation textures. Some clinopyroxenes show (sector-) zoning and green cores similar to that in the phenocrysts in the lavas.

Textural characteristics of clinopyroxenes

Three main zones are distinguished in most clinopyroxene phenocrysts (Fig. 2):

1. an outermost zoned brownish rim; grading into
2. a weakly zoned colorless mantle zone;
3. an anhedral to subhedral core, separated from the mantle by a sharp optical boundary.

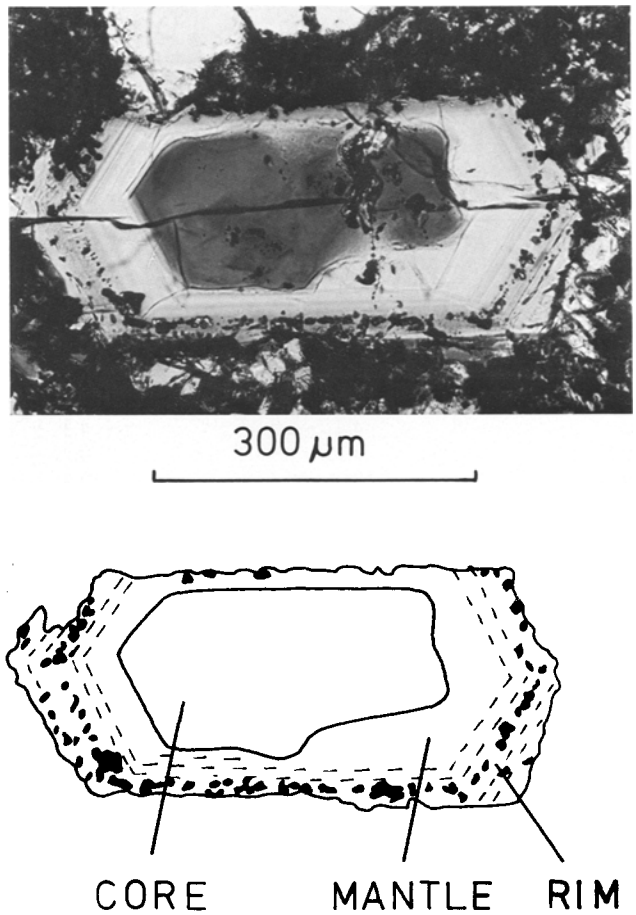

Fig. 2. Typical clinopyroxene phenocryst with characteristic core, mantle and rim zone

Rim and mantle zones

These zones occur in all clinopyroxene phenocrysts and microphenocrysts and are considered to be comagmatic. The brownish rim corresponds chemically to the groundmass clinopyroxenes. In glassy rocks the clinopyroxene phenocrysts lack the brownish rim but always show a colorless mantle zone, indicating that the mantle formed intratelluric ally. Rim and mantle zone dimensions are about 150 µm parallel and about 30 µm perpendicular to the c-axis. Inclusions of titanomagnetite and other groundmass phases such

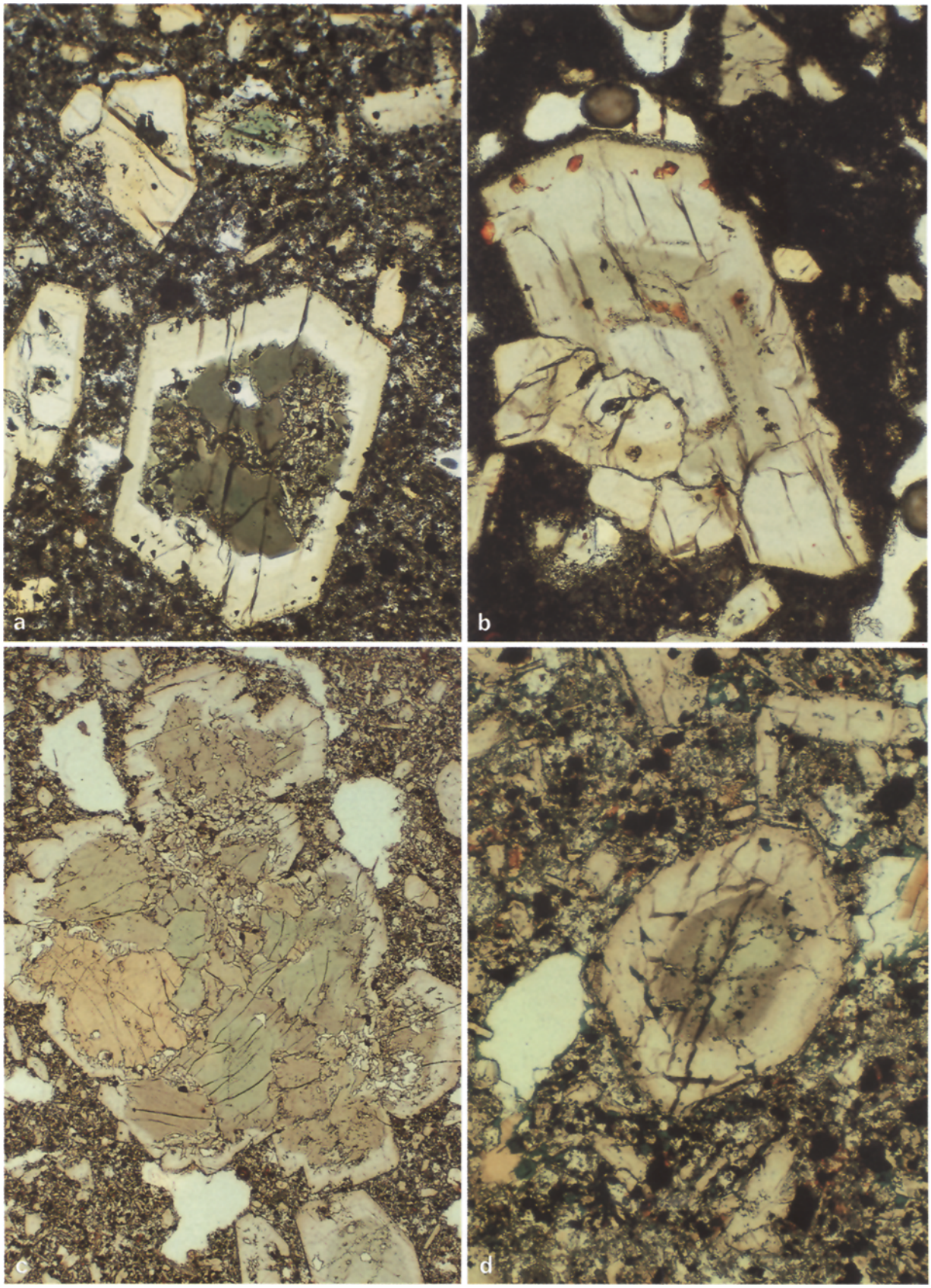

Fig. 3. a Three different clinopyroxene core types in foidite. Type a): gray-green/brownish (*top left*), type b): olive green (large crystal), type c): grass-green, strongly resorbed (*top right*). Width of field: 1 mm. **b** Clinopyroxene phenocryst with composite subhedral core: light inner core and dark green outer core. Width of field: 1 mm. **c** Disintegrating green clinopyroxene cumulate with common light mantle. Width of field: 2 mm. **d** Clinopyroxene phenocryst with composite green core: non-pleochroic pale green inner core (type c) and pleochroic olive green outer core (type b). See also Figure 8. Width of field: 1 mm

as apatite, hauyne, etc. and compositional zoning including sector-zoning are generally restricted to the rim zone.

Phenocryst cores

Shape, color and zoning of cores in the phenocrysts and some of the microphenocrysts is highly variable even within a single sample (Fig. 3a). Most cores are rounded or embayed indicating resorption prior to the mantle overgrowth. A few, however, are euhedral. Moreover, "composite" cores occur, which consist of an outer dark ring around an inner light-colored zone resembling the comagmatic mantle (Fig. 3b).

The cores are commonly darker than the surrounding comagmatic mantle zone and can be divided by their color into three main groups:

a) pleochroic gray-green/brownish cores,

b) pleochroic olive-green/ochre cores,

c) predominately non-pleochroic pale to grass-green cores.

In rocks from 152 eruptive centers studied in thin section, 90% of the foidites and basanites and 50% of the olivine nephelinites contain green clinopyroxene cores of type a) and b). Pale green clinopyroxene cores of type c) additionally occur in about 30% of the foidites. Core types a) and c) are distributed equally over the entire volcanic field with the exception of an olivine nephelinite group in the SE (Mosenberg group) and a basanite at the NE margin of the field near Boos which contain no green clinopyroxene at all. The dark green cores (type b) within the F-group are restricted in general to the center of the field coinciding with the spatial distribution of the intermediate rocks (MgO < 10 wt.%). There is, however, no clear correlation between clinopyroxene type and host rock composition (see below).

Cores of type a) and b), which cannot always be distinguished unambigously in thin section by optical methods, generally show patchy or concentric zoning, either normal or inverse. Resorption – causing a sieved core texture – seems to have taken place in some crystals subsequent to crystallization of the colorless comagmatic mantle because the resorption tubes now filled by matrix phases extend from the outside into the core (Fig. 4) and no intercalated resorption zone between core and mantle is observed.

Apatite, rare titanomagnetite, glass and very rarely phlogopite are found as inclusions. Tiny fluid, glass or opaque inclusions cannot be analyzed because of their small size (μm-range).

Most clinopyroxene cores consist of one crystal (diameter 50–2000 μm). In about 30% of the F-group samples studied, polycrystalline green clinopyroxene aggregates occur, the mantle zone of which has crystallized homoaxially to the core (Fig. 3c).

Pale green clinopyroxene cores (type c) are much less abundant and are unambiguously identified only in F-group rocks. They are smaller (usually less than 200 μm) and always strongly resorbed which is reflected by their anhedral shape, pronounced embayments and numerous tiny fluid (?) inclusions. Only one nephelinite contains a polycrystalline aggregate of type c) with apatite inclusions. Some clinopyroxene phenocrysts in F-group lavas contain a composite green core consisting of a pale green inner core of type c) and an olive-green outer core of type b) (Fig. 3d).

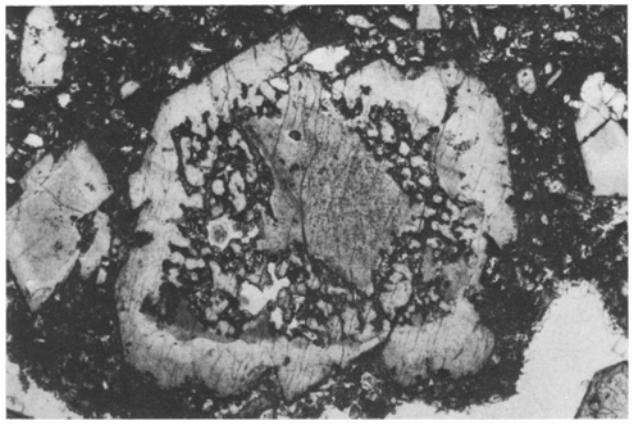

Fig. 4. Clinopyroxene phenocryst with strongly resorbed core in foidite. Corrosion started from the outside after or during crystallization of the light mantle zone. Width of field: 2.5 mm

Large single clinopyroxenes (megacrysts)

Large (a few mm to cm) single clinopyroxene crystals occur in tuff layers as well as in scoria and lavas of the F- and ONB-group. They are commonly euhedral, but many are strongly resorbed in the interior. They are composed of an optically relatively homogeneous gray-greenish core (like type a) and a narrow colorless mantle-rim zone. This sharp optical distinction between core and rim is characteristic of all large single clinopyroxenes.

Chemical characteristics of clinopyroxenes

Methods

Major element mineral analyses were performed with an ARL-SEMQ electron microprobe equipped with an energy dispersive system (KEVEX). Raw data were corrected according to Reed and Ware (1973). The Fe^{3+} content of the clinopyroxenes was calculated assuming stoichiometry. One clinopyroxene single crystal was analyzed for major elements by XRF; Fe^{2+} was determined by titration methods and yielded ideal stoichiometric composition.

The trace element composition of the clinopyroxenes was determined with a CAMECA IMS-3f ion-microprobe; the method is described by Shimizu (1981), Ray and Hart (1982) and Ray et al. (1983). The polished thin sections were gold-coated; the diameter of the analyzed spot was about 3–10 μm. Absolute concentrations were obtained for Sc, Ti, V, Cr and Sr.

Major elements

We have studied 66 samples (2–8 crystals in each sample) and analyzed 1–20 spots per crystal. Representative analyses are listed in Table 3. The data are evaluated in Figs. 5 to 7.

All clinopyroxenes are rich in Al, Ti, Fe^{3+} and Na (total about 15 atom%) and thus not well represented in the classic pyroxene quadrilateral diopside – enstatite – ferrosilite – hedenbergite. Therefore, the nomenclature proposed by Deer et al. (1978) and by Yagi and Onuma (1967) based on Si, Al and Ti concentrations was adopted in this study.

The mantle and rim compositions are titanaugites. These titanaugites and the green clinopyroxene cores in

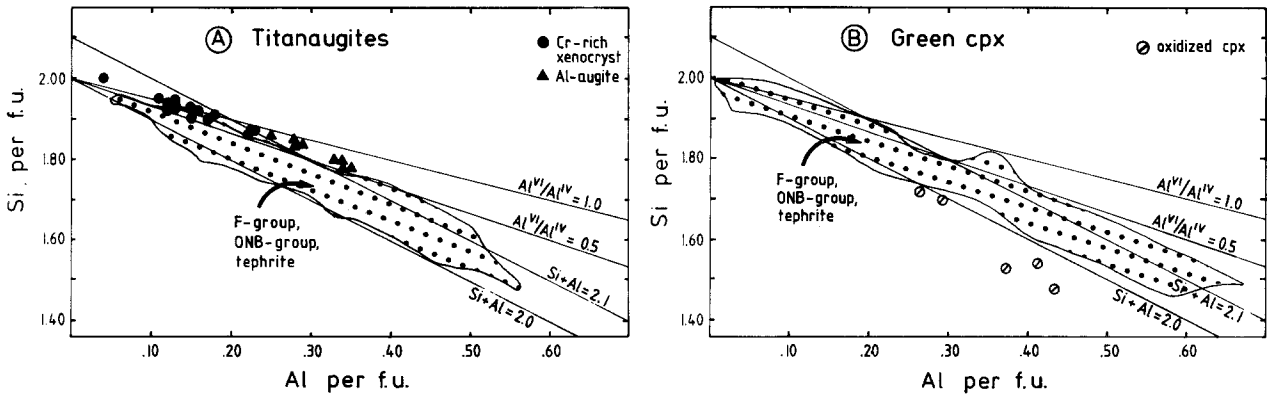

Fig. 5. Variation of atomic Si with atomic Al in titanaugites (**A**, 550 analyses) and green clinopyroxene cores (**B**, 450 analyses). Cr-rich xenocrysts and Al-augites as well as analyses of clearly oxidized parts in green clinopyroxenes are represented by individual symbols. Additionally, lines are given for octahedral Al=0 and 0.1 per f.u. and for Al^{VI}/Al^{IV} ratios of 0.5 and 1.0

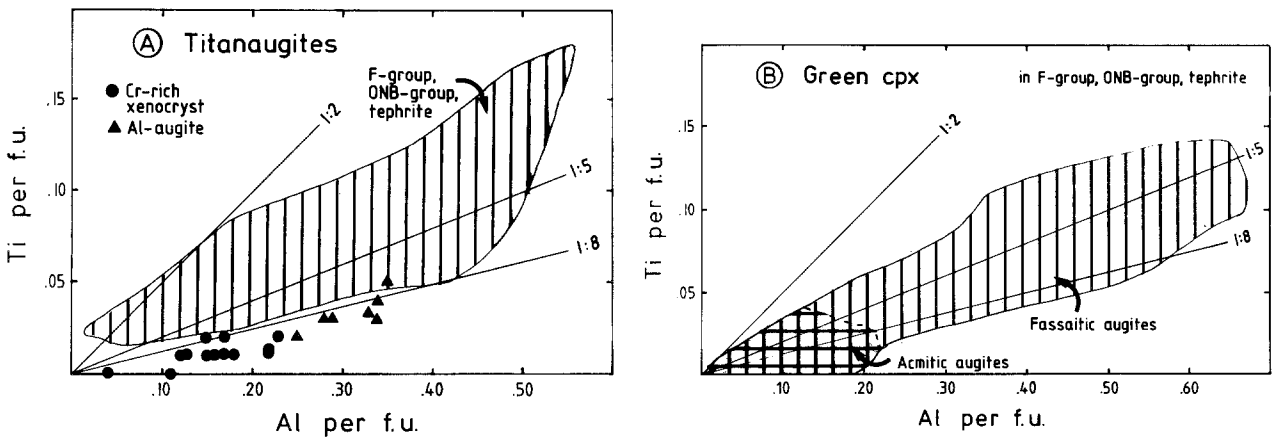

Fig. 6. Variation of atomic Ti with atomic Al in titanaugites (**A**, 550 analyses) and green clinopyroxene cores (**B**, 450 analyses). Cr-rich xenocrysts and Al-augites are represented by individual symbols. The green clinopyroxene analyses are subdivided into acmitic augites (150 analyses) and fassaitic, resp. other green augites (300 analyses). Additionally, lines of certain Ti/Al ratios are given

both magma groups show very similar crystal chemical substitution schemes (Figs. 5, 6): The Si-deficient tetrahedral sites are filled with Al with excess Al generally up to 0.1 per f.u. (formula unit) (Fig. 5). The titanaugite mantle-rim zonation corresponds to a decrease in Si (and Cr, Mg) and an increase in Al, Ti and Fe. Al^{VI}/Al^{IV} in titanaugites and green clinopyroxenes is commonly restricted to 0.5 and less, corresponding to the empirical classification „inclusions in basalts" by Aoki and Kushiro (1968). A strong Al excess over Ti in the Ti-pyroxene molecule Tp ($CaTiAl_2O_6$, Ti/Al=1/2) is evident from the Al-Ti variation diagram (Fig. 6). Probable additional clinopyroxene molecules are FAT ($CaFe^{3+}AlSiO_6$) and CAT ($CaAlAlSiO_6$).

The texturally defined clinopyroxene types are chemically best distinguished by their Al-Mg variation (Fig. 7): The titanaugites in mafic F-group and ONB-group magmas show restricted compositional variation. The green clinopyroxenes, in contrast, display lower Mg (and higher Fe) concentrations with variable Al values. Within the F-group magmas, the pleochroic (groups a and b) and non-pleochroic (group c) clinopyroxene cores differ in their Al content. In the pleochroic clinopyroxenes, therefore, a major part of Fe may be combined with Al to form the FAT molecule. These pyroxenes are thus termed "fassaitic augites". The Al-poor non-pleochroic clinopyroxene cores, in contrast, characteristically show high Na concentrations to form acmite; they are therefore called "acmitic augites". Both green pyroxene types contain very little Cr.

Chemically, there exists a transitional field between Mg-rich fassaitic augites and Al-rich titanaugites. Yet in every crystal studied, a clear inverse succession (i.e. Mg increase) between clinopyroxene core and mantle is observed. The same holds for the large single clinopyroxene crystals, the cores of which plot in the titanaugite and partly in the Mg-rich fassaitic augite field (Fig. 7).

Groundmass clinopyroxenes from one phonolite in the West Eifel are not plotted in this diagram (Fig. 7) because they are almost pure acmite (Table 3, 25. analysis) and thus distinct from the green cores and titanaugites. Clinopyroxene phenocrysts and microlites from phonolites in the East Eifel, e.g. Laacher See (Wörner and Schmincke, 1984) and Rieden (Viereck 1984), extend throughout the acmitic and fassaitic augite field (Fig. 7), but some show significantly higher acmite contents than the West Eifel green clinopyroxenes cores.

Colorless clinopyroxene cores are divided into "Cr-diopsides" with high Cr ($Cr_2O_3 > 0.6$ wt.%; Table 3) and relatively high Mg concentrations and "Al-augites" with

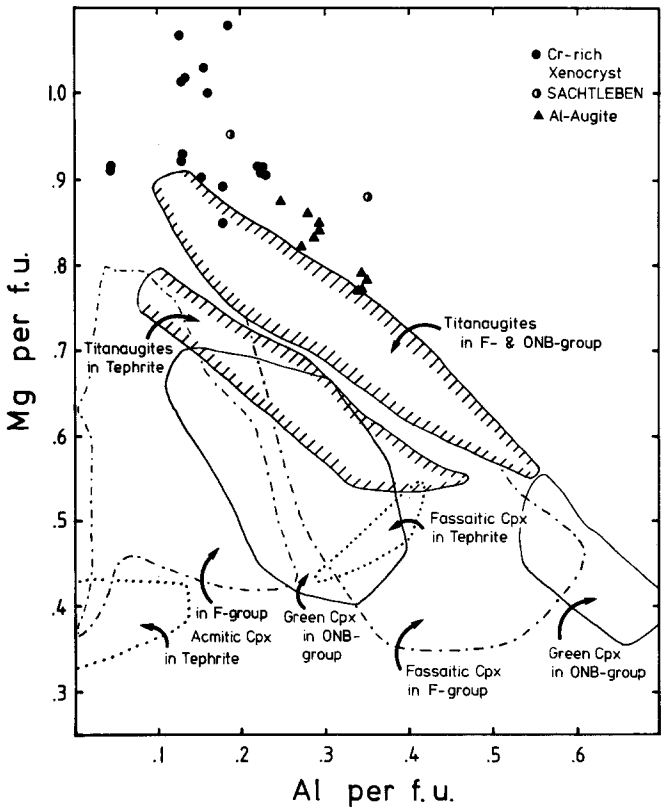

Fig. 7. Variation of atomic Mg with atomic Al in all clinopyroxenes studied (about 1000 analyses). The green clinopyroxenes in foidites and tephrites are divided into acmitic and fassaitic augites. The smaller field of green clinopyroxenes in ONB-group rocks characterizes analyses of two Al-rich crystals and is not supposed to define an additional subgroup. Cr-rich xenocrysts, Al-augites and for comparison Cr-diopside analyses from Sachtleben (1980) are represented by individual symbols

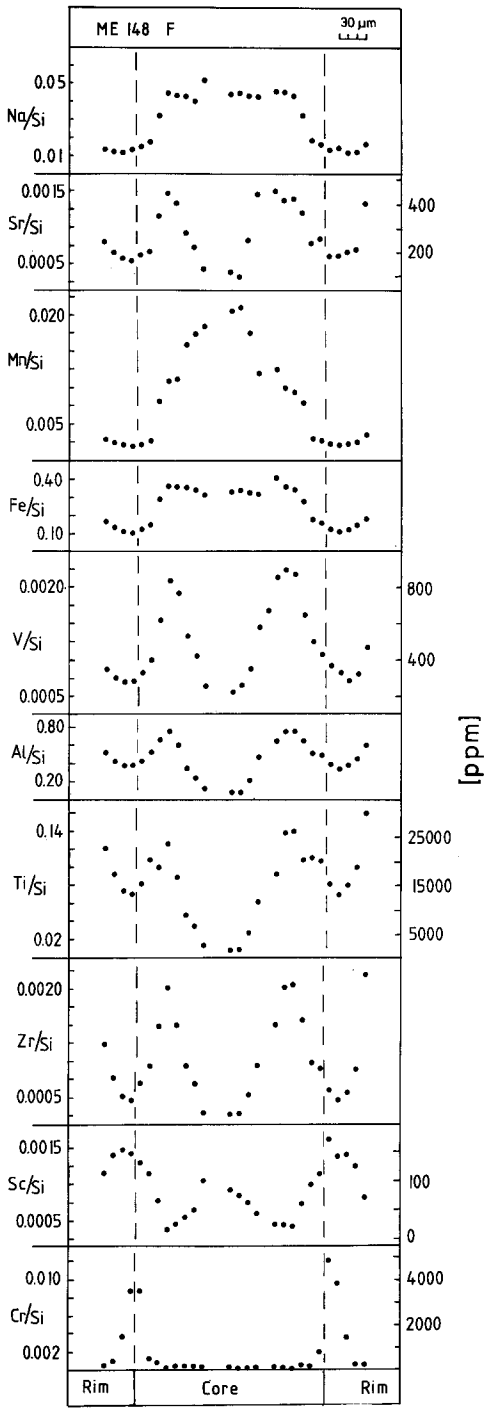

Fig. 8. Variation of relative secondary ion intensities across a clinopyroxene phenocryst with composite green core (same crystal as Fig. 3d). The symbol size comprises the statistical error

higher Al^{VI} (Fig. 5A) and lower Ca concentrations (<0.90 per f.u.; Table 3) than the titanaugites.

Trace elements

Trace element profiles across clinopyroxene phenocrysts support the above classification. Figure 8 shows a representative ion probe traverse across a clinopyroxene phenocryst with a composite green core. All profiles show a sharp chemical boundary between core and mantle: The inner clinopyroxene mantle is characterized by a pronounced peak and subsequent steep decrease in Cr content. Simultaneously, the incompatible elements – Na, Sr, Mn, Fe, V, Al, Ti, Zr – increase. The elemental decrease or increase is commonly stepwise rather than smooth. The titanaugite trace element profiles are interpreted by Duda and Shimizu (1985 and in prep.).

The homogeneous and inhomogeneous fassaitic cores always display higher incompatible and lower compatible (Cr, Sc) element concentrations. The acmitic cores, however, show high Na, Fe and Mn but low Sr, Al, Ti and Zr concentrations (Fig. 8).

A survey of all greenish clinopyroxene cores analyzed reveals a parallel trace element variation pattern for gray-green (i.e. Fe-poorer) and dark green (i.e. Fe-richer) fassaitic cores whereas the trace element variation within the acmitic series is very distinct (Fig. 9; Duda 1984). Moreover, fassaitic augites correspond to their titanaugitic mantle-rim zone in their trace element variation pattern.

Clinopyroxene crystallization

The textural characteristics and chemical diversity of the clinopyroxenes discussed above must reflect complex and diverse crystallization conditions. Thus, the clinopyroxene

Table 3. Representative single clinopyroxene analyses

Rock	F	F	F	F	F	ON	ON	B	Tert B	T	F	F	F	F	F
Spec.	ME 6	ME 6	ME 6	ME 38–4	ME 38–4	ME 143	ME 143	ME 76	ME 58–3	E 69	ME 47	ME 6	ME 6	ME 38–4	ME 38–4
Anal.	*6	*2	*1	*13	*36	*3	*1	*33	*11	*56	*37	*5	*14	*5	*3
Cryst.	PM	PM	PR	PM	GC	PM	PR	PC	AM	PC	MC	PC	PC	PC	PC
Type	Ti-Au	Ti-Au	Ti-Au	Ti-Au	Ti-Au	Ti-Au	Ti-Au	Ti-Au	Ti-Au		§	Fass	Fass	Fass	Fass
SiO_2	49.10	48.02	47.18	50.40	45.77	49.96	43.18	49.45	42.30	45.42	50.98	41.96	45.72	44.53	46.28
TiO_2	1.60	2.02	2.63	1.54	3.05	1.82	4.02	1.33	3.84	2.67	0.91	2.86	2.03	2.55	2.10
Al_2O_3	5.13	5.01	5.79	3.49	7.25	4.80	8.08	5.17	10.40	7.42	4.51	9.97	8.17	8.34	7.47
Cr_2O_3	0.35	–	–	0.36	0.27	0.27	–	0.92	0.12	–	–	–	–	–	–
Fe_2O_3	0.95	3.47	4.23	1.79	3.61	–	4.93	0.85	4.62	4.27	1.33	8.11	5.12	4.87	3.68
FeO	4.58	3.44	3.28	3.62	3.37	5.03	4.30	4.22	4.04	5.61	3.40	6.07	4.31	5.39	4.09
MnO	–	–	–	–	–	–	–	–	–	0.15	–	0.21	–	–	–
MgO	14.10	13.84	13.20	14.97	12.86	14.77	11.31	14.48	10.75	10.57	15.43	7.68	11.20	10.18	12.12
CaO	23.76	24.14	24.06	24.47	24.34	23.50	23.89	23.09	22.95	23.14	23.38	22.65	23.08	23.18	23.55
Na_2O	–	–	0.20	–	–	–	–	0.16	0.19	0.50	0.20	0.76	0.52	0.50	0.30
K_2O	–	0.07	0.07	–	–	0.13	0.06	–	0.06	0.06	–	0.08	0.08	–	–
Total	99.57	100.01	100.64	100.64	100.52	100.28	99.77	99.67	99.47	99.81	100.14	100.35	100.23	99.54	99.59
Cations on oxygen basis 6:															
Si	1.83	1.79	1.75	1.85	1.70	1.84	1.64	1.83	1.60	1.72	1.87	1.61	1.71	1.69	1.74
Al(IV)	0.17	0.21	0.25	0.15	0.30	0.16	0.36	0.17	0.40	0.28	0.13	0.39	0.29	0.31	0.26
Fe^{3+}(IV)	–	–	–	–	–	–	–	–	–	–	–	–	–	–	–
Ti	0.05	0.06	0.07	0.04	0.09	0.05	0.11	0.04	0.11	0.08	0.03	0.08	0.06	0.07	0.06
Al(VI)	0.05	0.01	–	–	0.02	0.05	–	0.06	0.06	0.05	0.06	0.06	0.07	0.06	0.07
Cr	0.01	–	–	0.01	0.01	0.01	–	0.03	–	–	–	–	–	–	–
Fe^{3+}(VI)	0.03	0.10	0.12	0.05	0.10	–	0.14	0.02	0.13	0.12	0.04	0.23	0.14	0.14	0.10
Fe^{2+}	0.14	0.11	0.10	0.11	0.11	0.15	0.14	0.13	0.13	0.18	0.10	0.19	0.14	0.17	0.13
Mn	–	–	–	–	–	–	–	–	–	0.01	–	0.01	–	–	–
Mg	0.78	0.77	0.73	0.82	0.71	0.81	0.64	0.80	0.62	0.60	0.84	0.44	0.63	0.58	0.68
Ca	0.94	0.96	0.96	0.96	0.97	0.93	0.97	0.91	0.93	0.94	0.92	0.93	0.92	0.94	0.94
Na	–	–	0.01	–	–	–	–	0.01	0.01	0.04	0.01	0.06	0.04	0.04	0.02
K	–	–	–	–	–	0.01	–	–		–	–	–	–	–	–
Total	4.00	4.01	3.99	3.99	4.01	4.01	4.00	4.00	3.99	4.01	4.00	4.00	4.00	4.00	4.00
Al(VI/IV)	0.29	0.05	–	–	0.07	0.31	–	0.35	0.15	0.18	0.46	0.15	0.24	0.19	0.27
Mg-No.	0.85	0.88	0.88	0.88	0.87	0.84	0.82	0.86	0.83	0.77	0.89	0.70	0.82	0.77	0.84
Fe^{3+}/Fe	0.18	0.48	0.55	0.31	0.48	–	0.50	0.13	0.50	0.40	0.29	0.55	0.50	0.45	0.43

§ intergrown with Fe-rich olivine

phenocryst harbor a wealth of information on the pre-eruption history of their host magmas. They are the most promising among all phenocryst mineral phases to infer evolutionary stages of the magmas. We will first discuss two types of cores whose interpretation is least controversial and proceed to discuss crystallization conditions of the titanaugite mantle and rim zones which are similar in all rocks studied. Finally, we will treat the fassaitic and acmitic cores in more detail because they are the most common type of green cores in alkali basalts, not only in the West Eifel magmas. Their origin is, however, least understood.

Cr-diopside

Texturally, these clinopyroxenes can be clearly recognized as xenocrysts by their anhedral shape and titanaugite rim. Chemically, they very much resemble clinopyroxenes from the peridotite xenoliths common in several West Eifel maar deposits (Sachtleben 1980; see also Frey and Green 1974 and Wass 1979a). They are, therefore, interpreted as fragments of peridotite xenoliths. Sr and Nd isotope studies of peridotite xenoliths from Dreiser Weiher/West Eifel (Stosch 1980; Stosch and Seck 1980) showed these nodules not to be cognate but accidentally entrained wall rock material. The xenoliths may represent fragments of the upper mantle at a depth not exceeding 50 km (Seck and Wedepohl 1983).

Al-augite

Al-augite cores are anhedral. In a polycrystalline aggregate with olivine they show a "modified igneous texture" as described by Wass (1979a). The characteristic low Ca and high Al, i.e. Al^{VI} contents but low Cr values compare well with the clinopyroxenes in the xenoliths of the Al-augite series and with high pressure natural and synthetic megacrysts (e.g. Binns et al. 1970; Green and Hibberson 1970; Irving 1974; Wilshire and Shervais 1975; Wass 1979a). In contrast to Cr-diopside xenocrysts, Al-augite megacrysts are generally believed to be cognate or at least to be related to contemporaneous magmatic activity. The main evidence is the similarity in the isotopic composition of clinopyroxene and host basalt (e.g. Stuckless and Irving 1976). Al-augites are thought to have formed at 10 to 20 kbar, i.e. within the uppermost mantle. No intergrowth between Cr-diopside and Al-augite is found in the Eifel lavas. The Cr-

Table 3 (continued)

Rock	F	ON	B	B	T	Alkpx	F	F	F	P	F	F	Alkpx	B	F
Spec.	ME 168	ME 143	ME 76	ME 58-3	E 69	R 31-1	ME 6	ME 132	ME 148	ME 185	D 2M	D 9	D 8	ME 169	ME 38-5
Anal.	*13	*34	*15	*12	*33	*2	*11	*20	*7	*21	*5	*1	*21	*6	*16
Cryst.	PC	PC	MC	AC	PC	MC	PC	AC	PC	GC	MC	AC	MC	AC	IC
Type	Fass	green	green	green	Fass		Acm	Acm	Acm		Mega	Mega	Al-Au	Al-Au	Cr-Di
SiO_2	39.86	38.10	46.62	47.25	44.91	41.80	49.96	51.61	51.76	50.79	50.99	45.12	48.60	49.95	51.83
TiO_2	3.44	4.70	2.11	1.78	1.32	3.14	0.24	–	0.14	1.43	0.96	2.57	1.30	1.05	0.57
Al_2O_3	13.53	14.45	6.75	5.48	6.49	10.63	3.06	2.22	0.61	0.89	3.44	8.12	7.64	6.60	3.57
Cr_2O_3	–	–	–	–	–	–	0.11	–	–	–	0.30	0.09	0.21	0.75	1.57
Fe_2O_3	6.82	5.59	4.76	6.81	7.73	7.33	2.83	4.05	4.46	26.50	1.24	4.82	1.48	0.76	–
FeO	4.79	6.78	6.88	7.22	8.19	6.49	10.27	6.60	11.96	–	4.17	4.01	3.80	4.16	3.01
MnO	–	–	–	1.47	0.43	0.19	0.52	0.46	0.55	3.13	–	–	–	–	–
MgO	7.71	6.91	9.55	9.73	7.40	7.23	9.04	11.11	9.22	0.49	15.14	11.42	13.85	15.19	16.39
CaO	23.44	23.00	21.73	19.48	22.08	22.78	22.57	21.91	19.94	3.88	23.14	23.38	21.53	20.52	21.71
Na_2O	0.45	–	1.28	2.34	1.03	0.88	0.89	1.46	1.62	11.56	0.22	0.39	0.70	0.68	0.62
K_2O	–	0.06	–	–	–	–	–	–	–	0.11	–	0.05	–	–	–
Total	100.10	100.39	99.68	99.66	99.58	100.47	99.49	99.42	100.26	98.78	99.60	99.97	99.11	99.66	99.27
Cations on oxygen basis 6:															
Si	1.52	1.46	1.77	1.81	1.74	1.60	1.92	1.95	1.98	1.98	1.89	1.69	1.80	1.83	1.90
Al(IV)	0.48	0.54	0.23	0.19	0.26	0.40	0.08	0.05	0.02	0.02	0.11	0.31	0.20	0.17	0.10
Fe^{3+}(IV)	–	–	–	–	–	–	–	–	–	–	–	–	–	–	–
Ti	0.10	0.14	0.06	0.05	0.04	0.09	0.01	–	–	0.04	0.03	0.07	0.04	0.03	0.02
Al(VI)	0.13	0.11	0.07	0.06	0.04	0.08	0.05	0.05	0.01	0.02	0.04	0.05	0.13	0.12	0.06
Cr	–	–	–	–	–	–	–	–	–	–	0.01	–	0.01	0.02	0.05
Fe^{3+}(VI)	0.20	0.16	0.14	0.20	0.23	0.21	0.08	0.12	0.13	0.78	0.03	0.14	0.04	0.02	–
Fe^{2+}	0.15	0.22	0.22	0.23	0.26	0.21	0.33	0.21	0.38	–	0.13	0.13	0.12	0.13	0.09
Mn	–	–	–	0.05	0.01	0.01	0.02	0.02	0.02	0.10	–	–	–	–	–
Mg	0.44	0.40	0.54	0.44	0.43	0.41	0.52	0.62	0.53	0.03	0.83	0.64	0.76	0.83	0.90
Ca	0.95	0.98	0.88	0.80	0.91	0.93	0.93	0.88	0.82	0.16	0.91	0.94	0.85	0.81	0.85
Na	0.03	–	0.09	0.17	0.08	0.07	0.07	0.11	0.12	0.87	0.02	0.03	0.05	0.05	0.04
K	–	–	–	–	–	–	–	–	–	0.01	–	–	–	–	–
Total	4.00	4.01	4.00	4.00	4.00	4.01	4.01	4.01	4.01	4.01	4.00	4.00	4.00	4.01	4.01
Al(VI/IV)	0.27	0.20	0.30	0.32	0.15	0.20	0.63	1.00	0.50	1.00	0.36	0.16	0.65	0.71	0.60
Mg-No.	0.75	0.65	0.71	0.66	0.62	0.66	0.61	0.75	0.58	–	0.86	0.83	0.86	0.86	0.91
Fe^{3+}/Fe	0.57	0.42	0.39	0.47	0.47	0.50	0.20	0.36	0.25	1.00	0.19	0.52	0.25	0.13	–

Rock: Alkpx Alkalipyroxenite; B Basanite; F Foidite; ON Olivine-Nephelinite; P Phonolite; T Tephrite; Tert Tertiary
Crystal: AC Aggregate/Center; AM Aggregate/Mantle; GC Groundmass crystal/Center; MC Megacryst/Center; PC Phenocryst/Center; PM Phenocryst/Mantle; PR Phenocryst/Rim

diopside xenocrysts, therefore, were probably taken up only by the final pulse otherwise they should have been occasionally overgrown by Al-augite.

Titanaugite

The continuous optical and chemical transition from the mantle to the rim zone, the latter corresponding compositionally to the groundmass clinopyroxenes, is clear evidence that the titanaugite zones are comagmatic. Chemically, the change from mantle to rim composition reflects the normal clinopyroxene evolution at decreasing pressure: increasing Al and Ti, decreasing Si and Mg (e.g. Wass 1979a).

If the depth of crystallization of the inner mantle zone can be determined, the result will provide a minimum pressure for the crystallization of all clinopyroxene cores. Therefore, equilibrium calculations were performed on the basis of the Mg/Fe distribution between clinopyroxene and melt and between clinopyroxene and olivine: For the F-group rocks and one olivine-nephelinite, Mg/Fe equilibrium distribution between clinopyroxene mantle and host basalt and between olivine phenocrysts and host basalt can be demonstrated using the equilibrium distribution coefficients (Roeder and Emslie 1970; Nielsen and Drake, 1979). Subsequently, equilibrium temperatures and pressures for clinopyroxene mantle, olivine and magma were estimated according to the method of Nicholls and Carmichael (1972) using a FORTRAN program given by Nicholls (1977). This calculation method utilizes the equilibrium distribution of the diopside component between clinopyroxene and magma and of the fayalite component between olivine and magma, respectively, as a function of pressure and temperature. The calculations yield temperatures of 1050° C to 1140° C and pressures of 5 to 10 kbar. Thus, the clinopyroxene mantle zone appears to have crystallized from the magma at depths corresponding to the lower crust down to the crust/mantle boundary.

In the basanites, clinopyroxene is preceeded by olivine. This is supported by the high Mg/Fe content of olivine compared to clinopyroxene. Moreover, the titanaugite trace

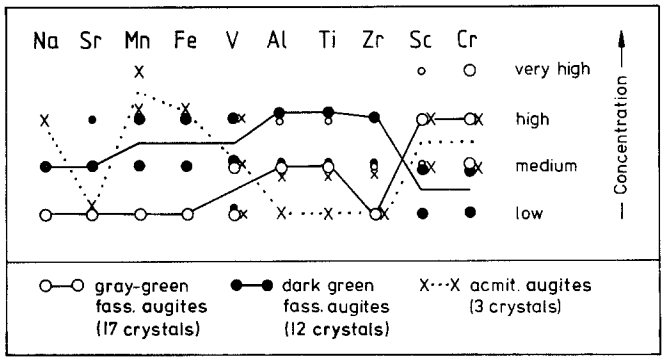

Fig. 9. Schematic distribution of minor and trace element contents in gray-green and dark green fassaitic and in acmitic cores. The symbol size corresponds to the number of analyses within one group.

element profiles in the basanites are generally simpler and show fewer steps than those in the F-group indicating a less complex crystallization history for the basanites. Titanaugite thus may have begun crystallization in the basanites at shallower depths than in the other groups.

The discontinuities in the titanaugite profiles (i.e. steps, 2. and 3. Cr and/or Sc peak and accompanying incompatible elements minima) might have been caused by the crystal coming into contact with more "primitive" melt: e.g. by crystal sinking or convective motion in the magma.

Fassaitic augite

The xenocrystic nature of fassaitic cores is reflected in the sharp optical and chemical boundary between core and titanaugite mantle, the resorption features and the high Fe/Mg ratio of the cores. But growth banding, partly subhedral shape and the absence of intergrowth with other phases like olivine, orthopyroxene, etc. suggest that they crystallized from a magma. It is thus unlikely that they originate from disintegrated wall rock xenoliths as postulated by Barton and Bergen (1981) or Lloyd (1981) for similar green cores in K-rich rocks from Leucite Hills, resp. Uganda (see below).

The composition of the host magma from which the fassaitic augites originally crystallized can only be deduced by means of the clinopyroxene composition in conjunction with assumed partition coefficients, and by the occurrence of some apatite and/or titanomagnetite inclusions. Major and trace element data show a similar distribution pattern in fassaitic and titanaugites but the fassaitic host magma must have been richer in incompatible elements, particularly in phosphorus and additionally in iron. Apatite never

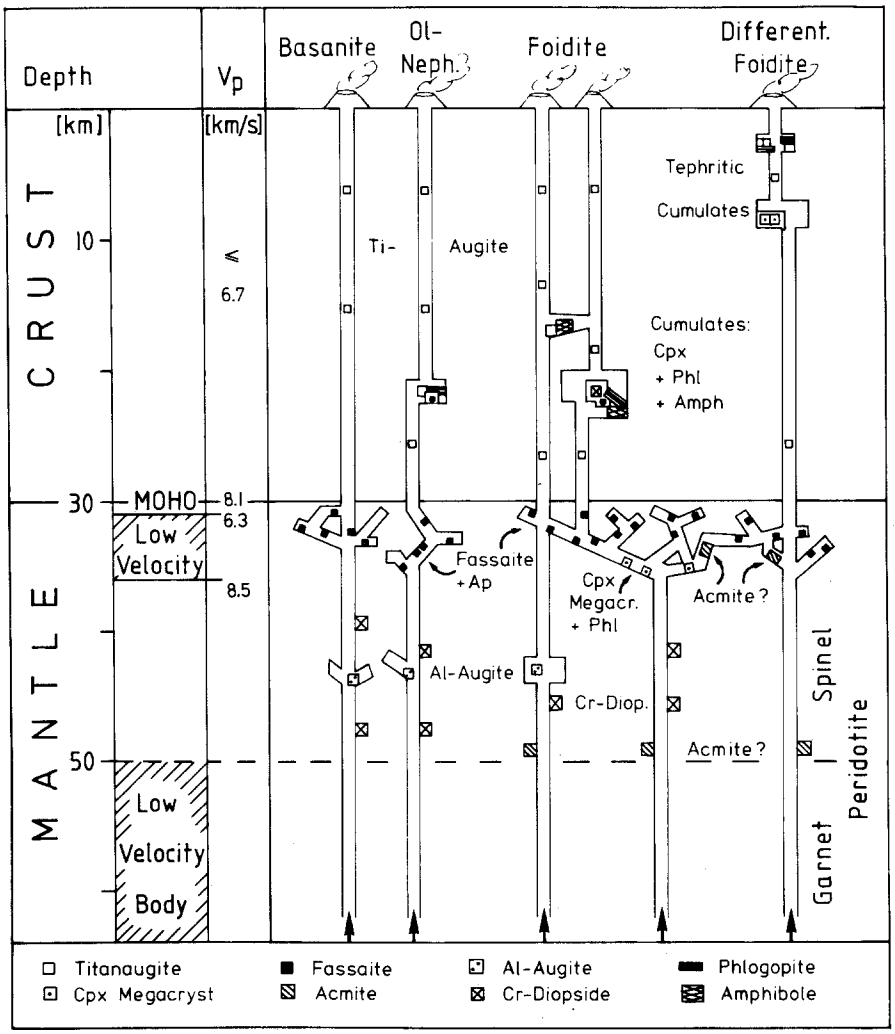

Fig. 10. Schematic cross-section through the lithosphere beneath the West Eifel showing estimated crystallization depths of the clinopyroxene types

occurs as inclusion in titanaugite mantle zones. Moreover, according to experimental (Watson 1980) and petrographic-geochemical investigations (Viereck 1984) apatite only starts to crystallize at P_2O_5 concentrations in the magma of at least 1 wt.%. REE and Sr data show as well that apatite is unlikely to crystallize from a mafic alkali basaltic magma (Irving and Frey 1984). Thus, the host magmas of fassaitic and titanaugite must have differed significantly in their composition and the change from a Fe-rich core to a Mg-rich mantle crystallization cannot only be due to a sudden change in oxygen fugacity (Mengel 1983) which would also contradict evidence for the xenocrystic nature of the fassaitic augites.

Because of the overgrowth relationship, the fassaitic augites must have formed at similar or higher pressures than the titanaugite mantle, i.e. at 15–30 km depth, possibly at the base of the crust. The striking diversity in composition of the cores within one thin section may be explained either by the influence of crystallization kinetics or, more likely, by every core crystallizing in a discrete magma batch of a certain degree of fractionation. The crystallization conditions were variable as reflected in a wide range of unzoned to normally and inversely zoned fassaitic augites.

Acmitic augite

The acmitic augites are texturally and chemically not in equilibrium with the magma from which titanaugite crystallized and are thus xenocrysts. The acmitic cores are generally very small, strongly resorbed and commonly lack any zonation or growth banding.

They contain apatite inclusions like the fassaitic augites, yet the trace element pattern is entirely different from the latter (Figs. 8, 9). Thus, if the acmitic cores crystallized from a similar magma as the fassaitic augites, its composition must have been changed drastically by e.g. precipitation of an Al-, Ti-, Sr- and Zr-fractionating phase which, however, has not been detected in the rocks studied.

The presumed depth of origin is the same as, or deeper than, the one for the fassaitic augites because of their overgrowth relationship (Fig. 8).

Discussion

We will now attempt to construct a consistent model of magma evolution and ascent beneath the West Eifel. At first, however, composition and hypotheses concerning the formation of green clinopyroxenes in other alkali basalt provinces are compared with the West Eifel data.

Green clinopyroxenes in other alkali basalt provinces

A world wide survey of green core clinopyroxenes in mafic alkali basalts was presented by Brooks and Printzlau (1978). They briefly discussed a number of theories proposed for the origin of the Fe-rich clinopyroxenes. Since then, additional detailed analytical studies were published (e.g. Wass 1979a; Barton and Bergen 1981; Lloyd 1981; Barton et al. 1982). Two main models for the origin of the green clinopyroxenes have been proposed:

a) The green clinopyroxene cores are regarded as cognate phases. The inverse zonation might be caused e.g. by increasing fo_2, possibly due to resorption of kaersutite at low pressure (Frisch and Schmincke 1969) or by sinking of the crystal in a convecting crustal magma chamber (Borley et al. 1971). According to Wilkinson (1975) and Wass (1979a) the green clinopyroxene cores represent a high pressure differentiation trend and the Mg-rich clinopyroxene mantles reflect prior crystallization of titanomagnetite.

b) The green clinopyroxenes are regarded as xenocrysts. They are thought to represent either wall rock debris entrained by the rising magma (b1) or crystallization products of an evolved magma (b2) which subsequently mixed with a more primitive magma.

The first possibility (b1) was invoked by Barton and Bergen (1981) to explain the occurrence of green clinopyroxene both as phenocryst cores and in ultramafic xenoliths in wyomingite lavas from Leucite Hills. The xenoliths are supposed to represent locally metasomatized upper mantle wall rock material which, however, is probably not the source material of the K-rich magmas. Lloyd (1981), on the other hand, suggests the salite – apatite – phlogopite nodules in alkalic lavas from SW-Uganda to represent the source rock, a completely metasomatized four phase-lherzolite, of the present host magma. Crystallization of Fe-rich clinopyroxenes in differentiated magmas and subsequent magma mixing (b2) was suggested e.g. by Thompson (1977) and Barton et al. (1982) to take place at crustal levels and e.g. by Brooks and Printzlau (1978), Wass (1979b) and Wass et al. (1980) at upper mantle levels.

The green clinopyroxenes in the West Eifel alkali basalts are regarded as xenocrysts (model b). For the fassaitic augites, we found crystallization conditions to differ distinctly from those in the present host magma and therefore favor the concept of formation in an evolved melt (b2). We are uncertain, however, if the acmitic augites represent wall rock debris (b1) or crystallization products of evolved melts (b2) like the fassaitic augites.

The comparison of the West Eifel clinopyroxenes with green clinopyroxenes in other alkali basalt provinces is difficult because often only average mineral analyses are given in the literature. Furthermore, chemical traverses across the crystal including the core/mantle boundary are rare or lack the diagnostic element Cr (e.g. Mengel 1983).

With respect to their Mg- and Al-contents, the clinopyroxenes from the literature show about the same variation as the West Eifel clinopyroxenes. It may be noted, however, that only those green augites which are interpreted to represent disintegrated mantle wall rock material and which now occur in ultrapotassic rocks (Barton and Bergen 1981; Lloyd 1981) correspond to the West Eifel acmitic augites with respect to Mg and Al. The Mg-Al concentration of the other Fe-rich augites from the literature shows no systematic correlation with the respective postulated crystallization process. The titanaugite mantle zones, however, compare surprisingly well in their Mg-Al variation with the West Eifel titanaugites.

A model of magma ascent in the West Eifel

The main conclusion from the foregoing discussion is that alkali basaltic magmas beneath the West Eifel did not rise to the surface immediately after generation in the mantle. Instead, some got stuck to form plutonic bodies upon cooling, while others remained largely fluid with shorter residence times in various reservoirs. Thus, we are faced with complex systems characterized by two main scenarios, which have also been put forward by Irving and Price (1981)

and Irving (1984): First, we must assume that differentiation of alkali basaltic magmas ranging from moderate to evolved compositions may take place at depth. Secondly, new batches of magmas, periodically rising from depth, percolate into, or flush through, the differentiating magma reservoirs, mixing with the partly differentiated liquid and/or entraining pyroxenes crystallized from the previous magma pulse. In order to sustain liquid reservoirs and the opportunity for such mixing to take place, either the same pathways and storage areas were used repeatedly – aided by preheating – or magma reservoirs in the upper mantle/basal crust are more common and/or of larger dimensions than represented by volume and distribution of the surface volcanics, or both.

Two types of recently acquired geophysical data are permissive but not sufficient evidence to independently assess generation and storage of magma beneath the West Eifel: A body characterized by 3–5% lower than normal P-wave velocities was detected at a depth of about 50 to 200 km below the West Eifel (Raikes 1980). The decreased seismic velocities in the 5×10^8 km^3 body were interpreted as due to the presence of about 1% partial melt. The F-group magmas and ONB-group magmas are believed to have been generated within this anomalous mantle region of the West Eifel (Mertes and Schmincke 1985). Another low velocity zone, about 3–6 km thick, was detected by refraction seismic studies just below the Moho in the Eifel (Mechie et al. 1983) with Vp = 6.3–7.0 km/s instead of the normal upper mantle velocities of Vp = 8.1–8.4 km/s. This low velocity zone could be accounted for by geologically young magmatic intrusions into, or metasomatic alteration of, the original upper mantle peridotite.

We thus envisage that in the Raikes' low velocity body, consisting of garnet peridotite, several percent of alkali basaltic magma rose through the overlying spinel peridotitic upper mantle to the Moho precipitating Al-augite in veins and pockets (Fig. 10). At the mantle/crust boundary, the magma spread into small discrete magma chambers or into a network of dikes. The magmas may have stagnated at that level because of the density contrast between mantle and crust. The alkali basaltic magma differentiated and precipitated eventually Fe-rich (fassaitic) clinopyroxenes and apatite. Stagnation in small magma chambers with subsequent filter pressing might be imagined as a likely fractionation mechanism. Yet, we think the "flow crystallization" mechanism proposed by Irving (1978, 1980) accounts more plausibly for the characteristic petrographic features observed in the West Eifel volcanics. In Irving's model, crystallization takes place from a flowing magma along the walls of narrow channels because magma chambers would be difficult to remain open at upper mantle pressures. In this scenario the precipitating liquidus phase will remain homogeneous at constant melt flow, but will display normal or inverse zonation at variable melt flow rates. The absence of cumulates of different phenocryst phases except fassaitic augite and apatite may be explained by this process as well, comparable to the telescoping precipitation of hydrothermal dike minerals. Periodic reaming of the partly-filled channels by energetic pulses of primitive magma would lead to the entrainment of single crystals and xenoliths, partial resorption and subsequent overgrowth by Mg-rich titanaugite once the magma had reached crustal levels.

Less Fe-rich fassaitic augites and the large single crystal clinopyroxenes (Mg-poor titanaugite) presumably crystallized at the beginning of the flow crystallization, i.e. deep in the dike network. The Fe-rich fassaite augites, however, originate, accordingly, from higher levels. One of the additional energetic new magma batches carrying Cr-diopside xenoliths and disintegrating Al-augite aggregates from greater depth (30–50 km) sampled several of the crystal-plated conduit walls and succeeded in rising into the crust. All entrained crystals and xenoliths were mantled by comagmatic titanaugite. The magma batches finally ascending to the surface in the West Eifel never exhibit clear geochemical fingerprints of mixing with evolved magmas at depth implying that the differentiated liquids were only small in volume and therefore "lost".

Within the crust, however, additional stagnation occurred to accumulate titanaugites with "older" cores, hornblende/or phlogopite, apatite, etc. (c.f. Becker 1977). In upper crustal reservoirs, magma differentiated locally towards tephrite and eventually phonolite magmas such as beneath the Laacher See volcano (Wörner and Schmincke 1984) and beneath the Rieden volcanic complex (Viereck 1984) in the East Eifel. These evolved magmas cannot, therefore, represent the host magmas of the green clinopyroxene cores and are thus quite distinct from Irving and Price's (1981) lherzolite xenoliths-bearing phonolitic lavas which supposedly formed at the crust/mantle boundary.

Metasomatized mantle xenoliths

Metasomatic alteration of mantle peridotite beneath continental and oceanic alkali basaltic provinces has been discussed repeatedly as a precursor to the formation of alkaline magmas. Geochemical studies have now shown that the source material must have been enriched in certain elements like Ti, Na, K, P, LREE, etc. in order to explain the chemical characteristics of the magmas (e.g. Menzies and Murthy 1980; Wass 1980; Wass and Rogers 1980; Mertes and Schmincke 1985). Additional evidence comes from partly metasomatized ultramafic xenoliths in alkali basalts.

For the West Eifel, Stosch (1980) proposed a metasomatic event of the upper mantle lherzolite, at most 150 Ma ago. The results, however, deny a genetic relation between these lherzolites and the alkali basaltic host magmas. Lloyd and Bailey (1975), on the other hand, in their pioneering study on mantle metasomatism, interpret the alkali pyroxenite xenoliths in the West Eifel (e.g. Weinfelder Maar) as the final product of complete metasomatic alteration of upper mantle peridotite. Our data show, however, that the two xenolith types are not genetically related. The alkali pyroxenites are clearly aggregates of liquidus phases of a magma similar to the present host magma as also postulated by Aoki and Kushiro (1968) and Becker (1977). This conclusion is based on textural (cumulus, no deformation textures in the alkali pyroxenites in contrast to the metasomatized peridotites, zoning in pyroxenes, etc.) and chemical evidence (high Cr- and low Ti-, K-contents in the peridotite amphiboles; c.f. Sachtleben 1980; Duda 1984). The alkali pyroxenite cumulates in several West Eifel localities, though, certainly require a more thorough study before they can be interpreted with more confidence.

Acknowledgements. This study forms part of A.D.'s Ph.D. thesis and was partly funded by the Bundesministerium für Forschung und Technologie, grant no. BMFT-ET 4236 A. The manuscript benefitted from critical comments by J. Hertogen, A. Irving, G.

Wörner. We thank O. Medenbach and A. Fischer for help with the photographic work, G. Olesch and E. Kessler for thin section preparation. We are especially grateful to H. Wänke (Max-Planck-Institut, Mainz) for generously allowing access to microprobe facilities.

References

Aoki K, Kushiro I (1968) Some clinopyroxenes from ultramafic inclusions in Dreiser Weiher, Eifel. Contrib Mineral Petrol 18:326–337

Barton M, Bergen vMJ (1981) Green clinopyroxenes and associated phases in a potassium-rich lava from the Leucite Hills, Wyoming. Contrib Mineral Petrol 77:101–114

Barton M, Varekamp JC, Bergen vMJ (1982) Complex zoning of clinopyroxenes in the lavas of Vulsini, Latium, Italy: evidence for magma mixing. J Volcanol Geotherm Res 14:361–388

Becker HJ (1977) Pyroxenites and hornblendites from the maar-type volcanoes of the Westeifel, Federal Republic of Germany. Contrib Mineral Petrol 65:45–52

Binns RA, Duggan MB, Wilkinson JFG (1970) High pressure megacrysts in alkaline lavas from Northeastern New South Wales. Am J Sci 269:132–168

Borley GD, Suddaby P, Scott P (1971) Some xenoliths from the alkalic rocks of Tenerife, Canary Islands. Contrib Mineral Petrol 31:102–114

Brooks CK, Printzlau I (1978) Magma mixing in mafic alkaline volcanic rocks: the evidence from relict phenocryst phases and other inclusions. J Volcanol Geotherm Res 4:315–331

Büchel G, Lorenz V (1982) Zum Alter des Maarvulkanismus der Westeifel. N Jahrb Geol Paläont Abh 163:1–22

Civetta L, Innocenti F, Lirer L, Manetti P, Munno R, Peccerillo A, Poli G, Serri G (1979) Serie potassica ed alta in potassio dei Monti Ernici (Lazio Meridoniale): Considerazioni petrologiche e geochimiche. Rend Soc It Mineral Petrol 35:227–249

Deer WA, Howie RA, Zusman J (1978) Rock-forming minerals. Vol. 2 Chain silicates. Longman, London, pp 1–668

Duda A (1984) Die petrologische Bedeutung der "Grünkern"-Pyroxene und anderer Einsprenglingsphasen in den Foiditen und Basaniten der Westeifel. Bochumer Geol Geotechn Arb 16:1–190

Duda A, Schmincke HU (1978) Quaternary basanites, melilite nephelinites and tephrites from the Laacher See area (Germany). N Jahrb Mineral Abh 132:1–33

Duda A, Shimizu N (1985) An application of kinetic crystal growth models to trace element zoning in alkali basaltic clinopyroxenes. Mater Sci Forum (in press)

Frey FA, Green DH (1974) The mineralogy, geochemistry and origin of lherzolite inclusions in Victorian basanites. Geochim Cosmochim Acta 38:1023–1059

Frisch T, Schmincke HU (1969) Petrology of clinopyroxene-amphibole inclusions from the Roque Nublo Volcanics, Gran Canaria, Canary Islands (Petrology of Roque Nublo Volcanics I). Bull Volcanol 33:1073–1088

Fuchs K, Gehlen vK, Mälzer H, Murawski H, Semmel A (eds) (1983) Plateau uplift – The Rhenish Shield – A case history. Springer, Berlin Heidelberg New York, pp 1–411

Green DH, Hibberson W (1970) Experimental duplication of conditions of precipitation of high pressure phenocrysts in a basaltic magma. Phys Earth Planet Interiors 3:247–254

Huckenholz HG (1965a) Der petrogenetische Werdegang der Klinopyroxene in den tertiären Vulkaniten der Hocheifel. I. Die Klinopyroxene der Alkaliolivinbasalt-Trachyt-Assoziation. Contrib Mineral Petrol 11:138–195

Huckenholz HG (1965b) Der petrogenetische Werdegang der Klinopyroxene in den tertiären Vulkaniten der Hocheifel. II. Die Klinopyroxene der Basanitoide. Contrib Mineral Petrol 11:415–448

Huckenholz HG (1966) Der petrogenetische Werdegang der Klinopyroxene in den tertiären Vulkaniten der Hocheifel. III. Die Klinopyroxene der Pikritbasalte (Ankaramite). Contrib Mineral Petrol 12:73–95

Huckenholz HG (1973) The origin of fassaitic augite in the alkali basalt suite of the Hocheifel area, Western Germany. Contrib Mineral Petrol 40:315–326

Irving AJ (1974) Megacrysts from the Newer Basalts and other basaltic rocks of SE Australia. Geol Soc Am Bull 85:1503–1514

Irving AJ (1978) Flow crystallization: A mechanism for fractionation of primary magmas at mantle pressures (abstr). EOS Am Geophys Union Trans 59:1214

Irving AJ (1980) Petrology and geochemistry of composite ultramafic xenoliths in alkalic basalts and implications for magmatic processes within the mantle. Am J Sci 280A:389–426

Irving AJ (1984) Polybaric mixing and fractionation of alkalic magmas; evidence from megacryst suites (abstr.) EOS Am Geophys Union Trans 65:1153

Irving AJ, Price RC (1981) Geochemistry and evolution of lherzolite-bearing phonolitic lavas from Nigeria, Australia, East Germany and New Zealand. Geochim Cosmochim Acta 45:1309–1320

Irving AJ, Frey FA (1984) Trace element abundances in megacrysts and their host basalts: Constraints on partition coefficients and megacryst genesis. Geochim Cosmochim Acta 48:1201–1221

Lloyd FE (1981) Upper-mantle metasomatism beneath a continental rift: clinopyroxenes in alkali mafic lavas and nodules from South West Uganda. Mineral Mag 44:315–323

Lloyd FE, Bailey DK (1975) Light element metasomatism of the continental mantle: The evidence and the consequences. In: Ahrens LH, Dawson JB, Duncan AR, Erlank AJ (eds) Physics and chemistry of the earth Vol. 9. Pergamon, Oxford, pp 389–416

Mechie J, Prodehl C, Fuchs K (1983) The long-range seismic refraction experiment in the Rhenish Massif. In: Fuchs K, Gehlen vK, Mälzer H, Murawski H, Semmel A (eds) Plateau uplift – The Rhenish Shield – A case history. Springer, Berlin Heidelberg New York, pp 260–275

Mengel K (1983) Petrographie und Geochemie der Tuffe des Habichtswaldes und seiner Umgebung (Nördliche Hessische Senke). N Jahrb Miner Abh 147:1–20

Menzies M, Murthy R (1980) Mantle metasomatism as a precursor to the genesis of alkaline magmas – isotopic evidence. Am J Sci 280A:622–638

Mertes H (1983) Aufbau und Genese des Westeifeler Vulkanfeldes. Bochumer Geol Geotechn Arb 9:1–415

Mertes H, Schmincke HU (1983) Age distribution of volcanoes in the West-Eifel. N Jahrb Geol Paläont Abh 166:260–293

Mertes H, Schmincke HU (1985) origin and differentiation of mafic potassic lavas of the Quaternary West Eifel volcanic field (FRG). I. Major and trace elements. Contrib Mineral Petrol 89:330–345

Nicholls J (1977) The activities of components in natural silicate melts. In: Fraser DG (ed) Thermodynamics in geology. D Reidel, Holland, pp 327–348

Nicholls J, Carmichael ISE (1972) The equilibration temperature and pressure of various lava types with spinel and garnet peridotite. Am Mineral 57:941–959

Nielsen RL, Drake MJ (1979) Pyroxene-melt equilibria. Geochim Cosmochim Acta 43:1259–1272

Raikes SA (1980) Teleseismic evidence for velocity heterogeneity beneath the Rhenish Massif. J Geophys 48:80–83

Ray GL, Hart SR (1982) Quantitative analysis of silicates by ion microprobe. Int J Mass Spec Ion Phys 44:231–255

Ray GL, Shimizu N, Hart SR (1983) An ion-microprobe study of the partitioning of trace elements between clinopyroxene and liquid in the system diopside – albite – anorthite. Geochim Cosmochim Acta 47:2131–2140

Reed SJB, Ware NG (1973) Quantitative electron microprobe analysis using a lithium drifted silicon detector. X-ray Spectrom 2:69–74

Roeder PL, Emslie RF (1970) Olivine-liquid equilibrium. Contrib Mineral Petrol 29:275–289

Sachtleben T (1980) Petrologie ultrabasischer Auswürflinge aus der Westeifel. Dissertation Univ Köln, 1–160

Seck HA, Wedepohl KH (1983) Mantle xenoliths in the Rhenish Massif and the Northern Hessian depression. In: Fuchs K, Gehlen vK, Mälzer H, Murawski H, Semmel A (eds) Plateau uplift – The Rhenish Shield – A case history. Springer, Berlin Heidelberg New York, pp 343–351

Shimizu N (1981) Trace element incorporation into growing augite phenocryst. Nature 289:575–577

Stosch HG (1980) Zur Geochemie der ultrabasischen Auswürflinge des Dreiser Weihers in der Westeifel: Hinweise auf die Evolution des kontinentalen oberen Erdmantels. Dissertation Univ Köln, 1–233

Stosch HG, Seck HA (1980) Geochemistry and mineralogy of the two spinel peridotite suites from Dreiser Weiher, West Germany. Geochim Cosmochim Acta 44:457–470

Stuckless JS, Irving AJ (1976) Strontium isotope geochemistry of megacrysts and host basalts from SE Australia. Geochim Cosmochim Acta 40:209–213

Thompson RN (1977) Primary basalts and magma genesis. III Alban Hills, Roman comagmatic province, Central Italy. Contrib Mineral Petrol 60:91–108

Viereck L (1984) Geologische und petrologische Entwicklung des pleistozänen Vulkankomplexes Rieden, Ost-Eifel. Bochumer Geol Geotechn Arb 17:1–337

Wass SY (1979a) Multiple origins of clinopyroxenes in alkali basaltic rocks. Lithos 12:115–132

Wass SY (1979b) Fractional crystallization in the mantle of late-stage kimberlitic liquids – evidence in xenoliths from the Kiama area, N.S.W., Australia. In: Boyd FR, Meyer HOA (eds) The mantle sample: Inclusions in kimberlites and other volcanics. Am Geophys Union, Washington DC, pp 266–373

Wass SY (1980) Geochemistry and origin of xenolith-bearing and related alkali basaltic rocks from the Southern Highlands, New South Wales, Australia. Am J Sci 280A:639–666

Wass SY, Rogers NW (1980) Mantle metasomatism – precursor to continental alkaline volcanism. Geochim Cosmochim Acta 44:1811–1823

Wass SY, Henderson P, Elliott CJ (1980) Chemical heterogeneity and metasomatism in the upper mantle: Evidence from rare earth and other elements in apatite-rich xenoliths in basaltic rocks from eastern Australia. Phil Trans R Soc Lond A 297:222–246

Watson EB (1980) Apatite and phosphorus in the mantle source regions: An experimental study of apatite/melt equilibria at pressures to 25 kbar. Earth Planet Sci Lett 51:322–335

Wilkinson JFG (1975) Ultramafic inclusions and high pressure megacrysts from a nephelinite sill, Nandewar Mountains, North-eastern New South Wales, and their bearing on the origin of certain ultramafic inclusions in alkaline volcanic rocks. Contrib Mineral Petrol 51:235–262

Wilshire HG, Shervais JW (1975) Al-augite and Cr-diopside ultramafic xenoliths in basaltic rocks from Western United States. In: Ahrens LW; Dawson JB, Duncan AR, Erlank AJ (eds) Physics and chemistry of the earth, vol. 9. Pergamon, Oxford, pp 257–272

Wörner G, Schmincke HU (1984) Mineralogy and geochemical evolution of the Laacher See magma chamber. J Petrol 25:805–835

Yagi K, Onuma K (1967) The join $CaMgSi_2O_6$ – $CaTiAl_2O_6$ and its bearing on the titanaugites. J Fac Sci Hokkaido Univ Ser IV 13:463–483

Received March 8, 1985 / Accepted June 28, 1985